

## CHARACTERIZATION OF RAT BONE MARROW LYMPHOID CELLS

### I. A STUDY OF THE DISTRIBUTION PARAMETERS OF SEDIMENTATION VELOCITY, VOLUME AND ELECTROPHORETIC MOBILITY

K. ZEILLER AND E. HANSEN

*Max-Planck-Institut für Biochemie, D-8033 Martinsried Am Klopferspitz, West Germany*

Received for publication September 15, 1977, and in revised form December 20, 1977 (MS 77-199)

Various cell populations in rat bone marrow were characterized by means of a two dimensional separation using velocity sedimentation and free flow electrophoresis and by electrical sizing of the separated cells. Up to 4.5 mm/hr five different populations with discrete distributions in volume (coefficient of variation 10% to 13%) and sedimentation velocity (coefficient of variation 6% to 10%) were observed. Three of the small sized populations represented lymphocytes and small normoblasts and two of the larger sized populations represented myeloid cells. Almost all of these cells were in the G<sub>0</sub>/G<sub>1</sub> cycle phase. In the faster sedimenting fractions which contained immature myeloid, erythroid and undefined blast cells and two S phase populations, discrete volume distributions were not evaluated. The cell populations with homogeneous volume (particularly the small lymphocytes) showed high density variations which considerably impair the separation resolution. The cells sedimenting slower than 3.5 mm/hr were further separated by means of free flow electrophoresis into three peaks differing in electrophoretic mobility (EPM). The peaks of low and high EPM contained two populations and the peak of medium EPM contained three populations all characterized by normal volume distributions of uniform coefficient of variation between 11% and 14%. The small cells in the peaks of high and medium EPM were normoblasts and the other cells were lymphocytes. The biological significance of these results is discussed.

The bone marrow, like most other organs, is a complex mixture of different cells which makes the investigation of single cell populations extremely difficult. A promising approach to overcoming this problem is offered by physical cell separation methods such as velocity sedimentation (14, 16), buoyant density centrifugation (8, 11) and free flow electrophoresis (29, 32) which have been shown to separate cells with discrete biological properties. The resolutions obtained may be considerably enhanced if different methods are combined. This is only useful, however, if the physical properties by which the cells are separated are independently distributed. In the following, a two step separation of bone marrow lymphocytes according to volume and electrophoretic mobility is described which shows that a two-dimensional separation can be achieved as a result of the uncorrelated variation of both variables. The separated cells were characterized on stained smears and by electrical sizing. By these means, various discrete lymphocyte populations were observed.

#### MATERIALS AND METHODS

**Animals and cells:** Bone marrow tissue from specific-pathogen-free (spf), 12 week old, inbred Wistar rats (ten animals per experiment were used) (Institut für Strahlenforschung, Neuherberg, Munich) was gently dispersed in TC solution Puck-G, supplemented with 1% deionized BSA. The cells were filtered through thin layers of cotton wool, washed twice and resuspended in the medium used in the next experimental step (see below). Care was taken to keep the cells at 4°C throughout the course of the experiments.

**Velocity sedimentation:** The cells were separated by means of velocity sedimentation according to Miller and Phillips (13). The technique was slightly modified as described in detail elsewhere (28). A gradient of calf serum, pH 7.4 (previously cross absorbed with rat spleen cells) was prepared with an electronic gradient mixer (Ultragrad, LKB), the serum concentration being 4% at the gradient surface, increasing steeply to 7%, and then linearly to 14% at the chamber base. The cells ( $5 \times 10^6$  cells per ml) were layered on top of the gradient as a 2-mm thick starting band and the gradient was fractionated after 10 hr. Cell viability was routinely tested before and after separation by trypan blue exclusion.

**Free flow electrophoresis:** Electrophoretic cell separations were performed with a free-flow electrophoresis apparatus FF 5 (Bender and Hobein, Munich, Germany), the conditions being described in detail elsewhere (30). To minimize cell damage, cells were exposed to the separation buffer (triethanolamine-glycine-medium) for no longer than 1 hr and immediately transferred into TC solution Puck-G-BSA. The cell viability was determined before and after separation by means of the trypan blue exclusion test.

**Cell sizing:** The cells were electrically sized by using the hydrodynamic focusing technique described by R. Thom *et al.* (22). The measurements were performed in a Metricell detector (10) using a cylindrical orifice 70  $\mu\text{m}$  in diameter, a suction of 0.3 kg/cm<sup>2</sup>, an aperture current of 1.2 mA, flow rates of 500 to 1000 particles per second and a temperature of 20°C. The cells were measured in TC solution Puck-G (0.31 osmol, pH 7.4). The symmetrical electrical pulses obtained were classified by a 256 multichannel analyser (AEG-Telefunken). Absolute volumes were calculated by calibrating the system with uniform polystyrene particles of 5  $\mu\text{m}$  and 7.9  $\mu\text{m}$  diameter (Particle Technology, Inc. Los Alamos, New Mexico).

**Data analysis:** The analysis of the data was performed with a 9820A Hewlett-Packard (HP) calculator (Hewlett-Packard Co., Palo Alto, Calif.) connected to a plotter or a Siemens (Siemens Corp., Iselin, N. J.) 4004-150 computer. The experimental volume profiles were standardized either to a relative area as 100% or to the same peak height. The volume profiles were approximated by normal distributions, fitting linear or log normal curves by means of an iterative trial and error method as recently described (24). The fitted single distributions, their sum and their parameters

were plotted. By knowing the distribution parameters, fittings were also performed with the HP calculator by varying the area of normal curves until the experimental and the calculated profile agreed visually. Distribution profiles were also analysed for the statistical moments of mean, variance, skewness and excess. The coefficient of variation (V.C.) was defined as the ratio of the standard deviation to the mean in percentage.

**Morphology:** The separated cells were suspended in fetal calf serum, smeared on slides, air dried, methanol fixed and Giemsa stained. Areas of the smeared cells were determined by means of a measuring grid at 800-fold magnification. The cell viability was tested by means of the trypan blue exclusion test.

**<sup>14</sup>C-Thymidine incorporation:** The cells ( $5 \times 10^6$  cells/ml) were suspended in TC medium RPMI (pH 7.2) supplemented with 10% fetal calf serum (Gibco, Grand Island, N. Y.) and incubated at 37°C in a CO<sub>2</sub> incubator (Forma Scientific, Marietta, Ohio). 0.285  $\mu\text{Ci}$  <sup>14</sup>C-thymidine (60 mCi/mMol; Radiochemical Centre, Amersham, England) were added to 1-ml fractions of these samples. After 2 hr, 1 ml of the thymidine labeled cell suspension was removed, TCA precipitated, filtered and the radioactivity measured in a Packard (Packard Instr., Downers Grove, Ill.) scintillation counter.

## RESULTS

**Velocity sedimentation profile of bone marrow cells:** In all experiments ( $n = 36$ ) the velocity sedimentation profiles of viable cells were bimodal with modes at 2.9 mm/hr and 5 mm/hr. (Fig. 1). A shoulder was observed in the total cell profile at 2.3 mm/hr as a result of the distribution of erythrocytes and nonviable cells.

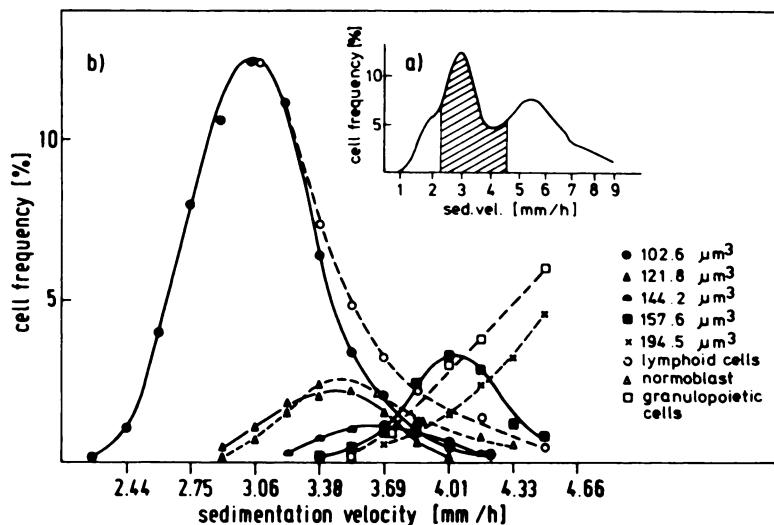


FIG. 1. Velocity sedimentation profile of rat bone marrow cells. a) Profile of all cells; b) Profiles of nucleated cells of different volume and morphology in the shaded area of profile a). The symbols of the size-defined cells are also used in Figure 4 and Table 1.

In the fractions sedimenting faster than 2.4 mm/hr, the cell viability was higher than 80%. The loss of nucleated cells during this separation step was approximately 30%.

#### Volume Analysis of Cells in the Sedimentation Profile

**Experimental errors:** The accuracy of electrical volume measurements is established for the hydrodynamic focusing technique and for viable leukocytes which behave as rigid, spherical and nonconductive particles when passing the measuring capillary (22, 10, 2, 9, 20, 23). Coincidence of the pulses was minimized by limiting the flow rate of cells to 500–1000 cells/sec. Residual errors may be caused by the formation of cell aggregates, by experimentally induced alterations in the physiological cell volumes or membrane conductivity and by contaminating nonviable cells. During the experiments erythrocytes, in contrast to leukocytes, aggregate to a considerable extent causing a distortion of the leukocyte volume profiles. This effect is demonstrated in Figure 2 in which freshly prepared erythrocytes show a single peak in the lower channels (plot 1), while erythrocytes which have aggregated after 12 hr storage at 4°C in the medium used in the 1g sedimentation show multimodal profiles (plot 2). These additional peaks are due to doublets, triplets etc. shown by the fact that: 1) the ratio of their

modes to that of the single erythrocytes was reproducibly  $2.03 \pm 0.05$ ,  $3.03 \pm 0.03$  and  $4.04 \pm 0.06$ ; 2) the relative proportions of distinct erythrocyte aggregates counted by phase contrast microscopy agreed with the relative areas of the respective peaks. Apparently disintegration of the aggregates during flow through the measuring orifice is negligible. Even vigorous pipetting barely reduced their number. All peaks could be accurately fitted by linear normal distributions independent of whether erythrocyte aggregations were measured after velocity sedimentation or electrophoresis. Thus the volume profiles of erythrocyte-contaminated leukocytes could be corrected by subtraction of singlets, doublets etc. from the experimental curve once their proportion was known from microscopical counts. We supposed that the error caused by this correction was smaller than that caused by chemical or physical removal of red cells.

We also considered the possibility of error arising from changes in the physiological volume or membrane conductivity of viable leukocytes during the course of the separation. The change in volume was analysed by storing bone marrow or lymph node cells in the 1-g separation medium for 12 hr at 4°C. Bone marrow cells were trimodally distributed with the erythrocytes in peak I (Fig. 3). After storage, peak II (which was corrected for erythrocyte aggregates), consisting mainly of lymphoid cells (see later), showed an

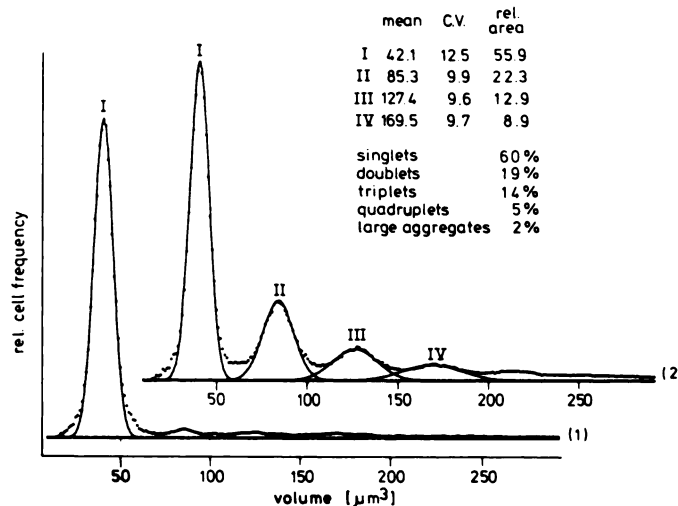


FIG. 2. Volume distribution profiles of rat erythrocytes immediately after preparation (plot 1) and after 12-hr storage at 4°C in TC solution Puck-G supplemented with 8% calf serum (plot 2). The profiles of  $10^5$  cells were standardized to the same height as peak I. The erythrocyte aggregates were evaluated by phase contrast microscopy. The experimental profiles (dots) could be closely approximated by linear normal distributions (solid lines) the distribution parameters of which are shown.

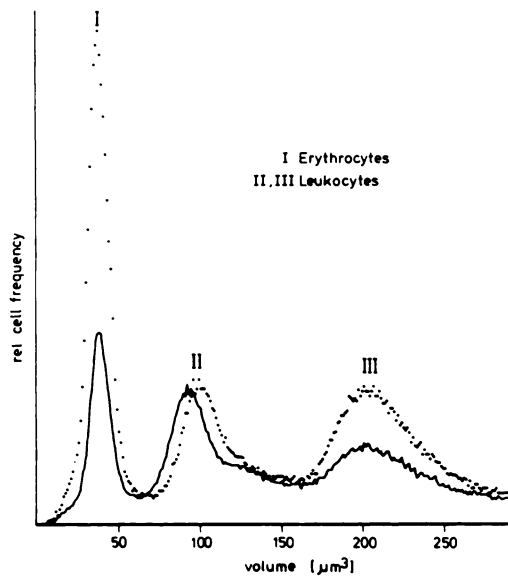


FIG. 3. Volume distribution profiles of rat bone marrow cells immediately after preparation (dotted lines) and after 12-hr storage (solid lines) at 4°C in TC solution Puck-G supplemented with 8% calf serum. The profiles of  $10^5$  cells were standardized to the same height as peak II.

average volume decrease of 8%. The relative areas of peaks I and III decreased, which is best explained by erythrocyte loss through aggregation and some selective cell loss in the larger cells. Similar alterations were observed in lymph node cells. In conclusion it seems that the small volume alterations are rather uniform for all cells, which is in agreement with the finding of other authors (4, 7). Thus errors caused by artificial distortions of physiological volume distributions can be disregarded.

Distortions also result from the contribution of nonviable cells. Experience shows that a decrease in cell viability is correlated with a tailing of volume profiles to the higher channels. At cell viabilities higher than 80%, single symmetrical profiles will not be seriously affected. However, in multimodal profiles, the peaks in the higher channels will be slightly distorted by the tails of the previous peaks. Since corrections are not possible, approximations of skews by normal distributions must be regarded critically.

#### *Fitting of Normal Distributions to the Volume Profiles*

Volume distributions of nucleated cells were determined in successive fractions of the BM

sedimentation profile as shown in the perspective plot in Figure 4a. A comparison of these plots revealed the following characteristics: 1) Average cell volumes and sedimentation velocities were correlated as expected. 2) Up to 4.5 mm/hr, the volume distributions showed discrete peaks and shoulders at rather constant positions. In the slowly sedimenting fractions, peak I was dominant. With increasing sedimentation velocity, this peak decreased while peak II and III grew until peak III was dominant at 4.5 mm/hr. 3) Over 4.5 mm/hr peak III was continuously shifted with sedimentation velocity to the higher channels simultaneously showing an increasing positive skew (not shown in Fig. 4a). The discreteness of the volume profiles up to 4.5 mm/hr suggested that various cell populations might be characterized by a) fitting normal distributions to the volume profiles and b) using the proportion of cells under single fitted curves to calculate the sedimentation profile of these volume-defined cells. Normal distributions were fitted according to Valet *et al.* (24). These fits were only slightly distorted by erythrocyte aggregates and nonviable cells in the fractions faster than 2.6 mm/hr. Up to 4.5 mm/hr, at least five different distributions were obtained by fitting log normal curves, the coefficients of variation of which ranged between 10% and 13% (Fig. 4b, Table 1). The goodness of fit is demonstrated in Figure 4a where the superpositions of the fitted curves (solid line) well agree with the experimental profiles (dotted line). In general approximations with log, normal curves gave better fits than linear normal curves but since the coefficients of variation are relatively small this can be disregarded.

The medians and V.C.'s of the single fitted distributions were reasonably constant over a series of successive fractions (Table 1). Only the relative areas under these curves changed continuously with sedimentation velocity growing to a maximum and then decaying. As pointed out previously, some errors result from the contribution of nonviable cells (data in parentheses in Table 1). However these may be disregarded in successive fractions in which the area of fitted curves shows continuous change.

#### *Characterization of Cell Populations by Volume and Sedimentation Velocity*

The portion of volume defined cells in the different fractions of the velocity sedimentation

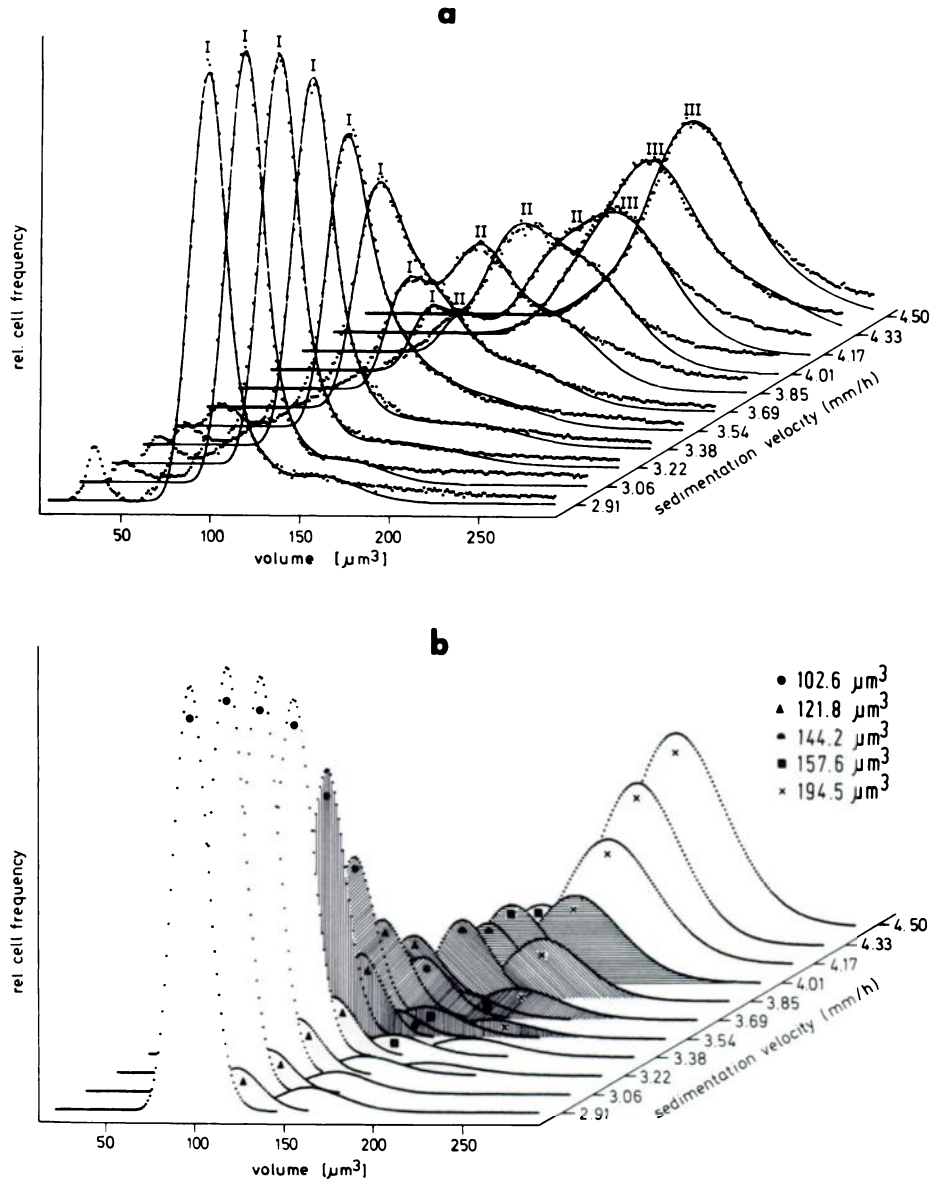


FIG. 4a and b. Volume distributions of nucleated bone marrow cells of different sedimentation velocities. All experimental profiles were standardized to a relative area of 100%. a) Experimental profiles (dotted lines) and superpositions of the fitted log normal curves (solid lines) shown in b). b) Distribution of single log normal curves fitted to the experimental volume profiles. For symbols see Table 1.

profile was calculated from the areas of fitted curves and plotted against sedimentation velocity (Fig. 1). It appeared that the cells with median volumes of 102.6  $\mu\text{m}^3$ , 121.8  $\mu\text{m}^3$ , 144.2  $\mu\text{m}^3$  and 157.6  $\mu\text{m}^3$  sedimented each as a discrete symmetrical band with modes at 3.06 mm/hr, 3.46 mm/hr, 3.69 mm/hr and 4.04 mm/hr, re-

spectively. Thus it seems that small bone marrow cells show different clusters of discrete distributions in volume and sedimentation velocity. A calculation of the V.C. of the single sedimentation profiles revealed values of about 10% for the smallest cells and about 6% for the three larger cells. These sedimentation dispersions are

TABLE I  
Volume Distribution Parameters of Log Normal Curves Fitted to the Experimental Profiles Shown in Figure 4<sup>a</sup>

Sedimentation Velocity mm/hr	Cell Volumes ( $\mu\text{m}^3$ )											
	M.	V.C.	A.	M.	V.C.	A.	M.	V.C.	A.	M.	V.C.	A.
2.91	99.4	9.8	80.1	126.3	10.2	(10.9)	167.2	11.2	(9.0)			
3.06	102.3	9.7	81.4	126.3	10.2	(10.9)	164.8	11.2	(7.7)			
3.22	103.5	9.6	74.4	125.1	10.3	(13.6)	163.7	11.4	(6.6)	198.7	11.8	(5.4)
3.38	104.6	10.1	70.0	126.3	10.1	(14.3)	161.3	11.6	(7.6)	204.6	11.4	(8.1)
3.54	105.8	9.8	53.3	125.1	9.8	19.5	143.8	9.8	7.4	198.7	11.8	(8.2)
3.69	104.0	11.2	34.1	120.4	12.1	26.1	142.6	10.7	17.1	196.4	11.9	(13.0)
3.85	102.9	10.2	14.6	120.4	12.1	18.3	147.3	10.3	23.8	192.9	11.5	26.6
4.01	100.5	10.5	9.6	120.4	12.6	8.2	143.8	10.6	16.6	194.1	12.7	39.0
4.17	100.5	10.5	6.4	120.4	12.6	4.5	143.8	10.6	6.4	195.2	13.2	61.4
4.33 <sup>+</sup>				123.9	11.3	1.5	143.8	10.2	3.1	192.9	12.1	64.5
4.50 <sup>+</sup>							143.8	10.2	4.8	197.6	13.3	87.3

<sup>a</sup> The symbols are used in the Figures 1 and 4: M = linear median of volume; V.C. = coefficient of variation in %; A = relative area of the curves. Areas in parentheses are incorrect due to experimental errors (see text). +) The sum of the areas of the fitted curves is less than 100% due to the appearance of a positive skew in the high channels.

considerably larger than those observed with plastic particles of similar size variations but uniform density (13, 28).

#### Morphological Characterization of Cells in the Sedimentation Profile

The separated cells were classified on Giemsa stained smears and their proportion in the different fractions was plotted against sedimentation velocity. Up to 4.5 mm/hr modal distributions of three different cell lines were identified: lymphoid cells between 2.4 mm/hr and 4.3 mm/hr, small normoblasts between 2.9 mm/hr and 4.1 mm/hr and myeloid cells in the fractions faster than 3.6 mm/hr. (Fig. 1). The lymphoid cell profile showed a pronounced positive skew and the proportion of lymphocytes with large cell diameters was higher in the faster than in the slower fractions.

A comparison of the sedimentation profiles of morphologically and volume-defined cells suggested that most of the  $157.6 \mu\text{m}^3$  and  $194.5 \mu\text{m}^3$  cells represent cells of the myeloid series and most of the  $102.6 \mu\text{m}^3$  cells represent small lymphocytes. On the other hand, the  $121.8 \mu\text{m}^3$  and  $144.2 \mu\text{m}^3$  cells could not be clearly correlated with morphologically characteristic cells. This results from the fact that small normoblasts show cell diameters similar to the smallest lymphocytes on the smears but show good coincidence in their sedimentation profile with the  $121.8 \mu\text{m}^3$  cells (Fig. 1). Since volume measurements of electrophoretically separated cells also suggest (see later) that normoblasts possess small volumes, it seems likely that they contribute to the distribution of the  $102.6 \mu\text{m}^3$  cells and partially cause their high sedimentation dispersion as a result of higher cell density. In this case, the  $121.8 \mu\text{m}^3$  and  $144.2 \mu\text{m}^3$  cells would represent lymphoid cells.

These results indicate that 1) different marrow cell lines show characteristic and discrete volume distributions and 2) that within these lines differences in cell volume are in most cases too small to allow resolution with the 1 g separation technique.

#### Electrophoretic Separation of Slowly Sedimenting Cells

Bone marrow cells sedimenting between 2.6 mm/hr and 3.5 mm/hr were further separated by free-flow electrophoresis. This sequence was used because prior enrichment of cell classes by

velocity sedimentation results in a shortening of the electrophoretic separation time and thus a better preservation of the cell viability (30). Alterations of the net negative surface charge during sedimentation were not observed: bone marrow leukocytes which were freshly prepared or stored in the velocity sedimentation medium for 12 hr at 4°C showed identical electrophoretic profiles.

In all experiments, cells with a sedimentation velocity of 2.6 mm/hr to 3.5 mm/hr showed a trimodal electrophoretic separation profile (Fig. 5). Most of the cells migrated with low electrophoretic mobility. The cell viability ranged between 80% and 90%, slightly lower in the faster fractions. Approximately 20% of the cells were lost during this separation step, a process which seemed to be random as suggested by the similarity of the volume profiles of all cells before and after separation. If cells of sedimentation velocity slower than 3 mm/hr were separated, the peak of medium electrophoretic mobility decreased.

#### *Volume Analysis of Cells in the Electrophoretic Profile*

**Experimental errors:** A comparison of the volume profiles of all cells before and after electrophoresis showed an average volume decrease of about 7% suggesting that artificial volume changes can be disregarded. The contribution of the nonviable cells to the volume profiles is negligible. Considerable distortions however were observed in the faster fractions due to erythrocyte aggregates. Here the volume profiles had to be corrected as previously described.

#### *Fitting of Normal Distributions to the Volume Profiles*

Volume distributions were determined in successive fractions of the electrophoretic profile and corrected for erythrocyte aggregates. A comparison of these profiles in Figure 6a shows discrete peaks and shoulders, the position of which seems to be constant in successive fractions.

The discreteness of the volume profiles enabled fitting of normal distributions. In all cases the best approximations were obtained with log normal curves two of which fitted the profiles in the fractions of high and low EPM, while three fitted the profiles in the fractions of medium EPM (Fig. 6b).

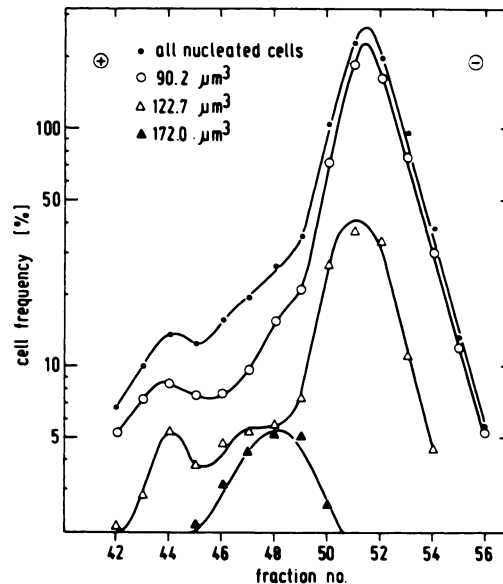


FIG. 5. Electrophoretic profile of nucleated bone marrow cells sedimenting between 2.6 mm/hr and 3.5 mm/hr. The profiles of cells of discrete volume distributions (see Fig. 6 and Table 2) are shown.

A comparison of the distribution parameters of the fitted curves listed in Table 2 revealed that: 1) all fitted curves showed V.C.'s between 11% and 14%, and 2) the median volumes of the small and medium sized cells were similar within each range of high, medium and low EPM but were slightly different between these ranges. This suggests that the dispersion in volume may characterize various different cell populations in the electrophoretic profiles.

#### *Characterization of Cell Populations by Volume and EPM*

The portion of cells with a distinct volume dispersion, calculated from the relative areas under the fitted curves and the actual cell frequency in the electrophoretic fractions, was plotted against the electrophoretic fraction number (Fig. 5). Since the volume differences within the small and medium sized cell classes in the different electrophoretic ranges were too small to allow precise discriminations in the region of overlap (fractions 46 and 50) they were each plotted as a single cell class in Figure 5. The resulting electrophoretic profiles were trimodal for both the small and the medium sized cells. The larger cells were symmetrically distributed in the fractions of medium EPM. These results

suggest that 1) variations in volume and EPM are independent and 2) at least seven different cell populations are described by these properties in the sedimentation range between 2.6 mm/hr and 3.5 mm/hr. Thus the two dimensional separation by velocity sedimentation and free flow electrophoresis seems to considerably enhance the separation resolution.

#### Morphological Characterization

The biological significance of the volume-defined cell populations in the electrophoretic frac-

tions was further analyzed in fractions 44, 48 and 52 (Fig. 5) by comparing the area and morphology of Giemsa stained cells on dried and fixed smears. In the fractions 44 and 52, the cell area histograms were bimodal, most of the cells being small (Fig. 7). In fraction 48 the area histogram, in addition to the small cells, showed larger cells and seemed to be trimodal. Thus the area histograms of smeared cells roughly correlated with the volume profiles in the respective fractions.

Discrete size distributions could also be correlated with morphologically characteristic cells,

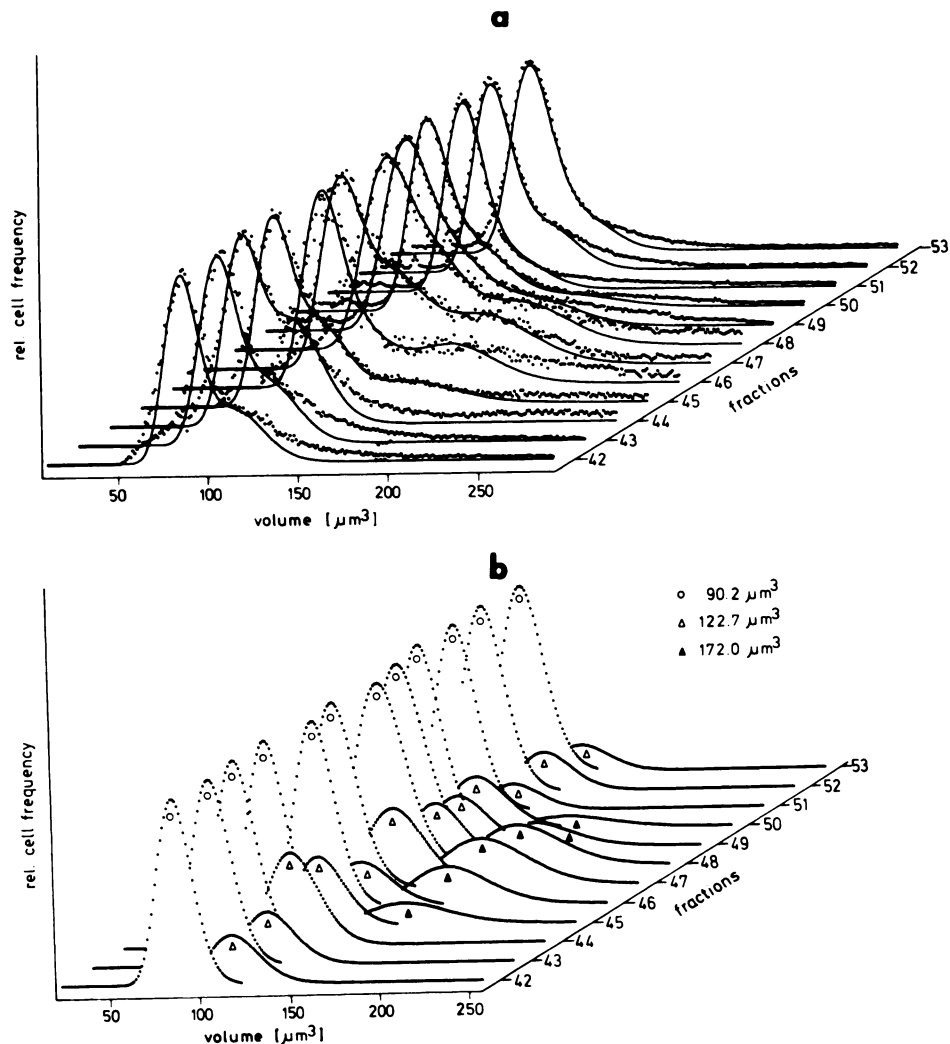


FIG. 6a and b. Volume distribution profiles of nucleated bone marrow cells of different electrophoretic mobility shown in Figure 5. All experimental profiles were standardized to the same height as the highest peak. a) Experimental profiles (dotted lines) and superpositions of the fitted log normal curves (solid lines) shown in b). b) Distribution of single log normal curves fitted to the experimental volume profiles. For symbols see Table 2.



TABLE II  
*Volume Distribution Parameters of Log Normal Curves Fitted to the Experimental Profiles Shown in Figure 6<sup>a</sup>*

Electrophoretic Fraction No.	Cell Volume ( $\mu\text{m}^3$ )								
	○			△			▲		
	M.	V.C.	A.	M.	V.C.	A.	M.	V.C.	A.
42	87.7	11.2	74.4	120.4	11.9	25.6			
43	91.2	12.1	71.3	122.7	11.6	28.7			
44	86.5	11.8	62.0	115.7	11.9	38.0			
45	87.7	12.3	56.9	116.9	11.8	28.4	167.2	14.0	14.7
46	97.0	11.4	49.8	123.9	13.2	29.7	173.0	12.8	20.5
47	91.2	13.4	50.5	125.5	13.3	27.0	173.0	12.3	22.5
48	98.2	14.5	59.3	130.9	12.0	20.7	177.7	13.3	20.0
49	92.4	15.2	64.1	127.4	12.8	21.4	170.7	12.3	14.5
50	86.5	12.6	65.9	120.4	13.3	25.1	170.7	14.0	8.9
51	86.5	13.0	84.2	121.6	12.1	15.8			
52	86.5	13.2	79.3	121.6	12.1	20.7			
53	91.2	13.2	85.0	125.1	11.7	15.0			

<sup>a</sup> The symbols are used in Figures 5 and 6: M = linear median of volume; A = relative area of the fitted curves; V.C. = coefficient of variation.

particularly in the fractions of high and low EPM. In fraction 44, all small sized cells were normoblasts showing a modal distribution in the area histogram (Fig. 7). The larger cells were all medium sized and rather uniform lymphocytes with little cytoplasm (Fig. 8a). In fraction 52, all cells were lymphocytes which fall into two classes (Fig. 8c). The small lymphocytes showed a dense nucleus and hardly visible cytoplasm. The larger cells showed a lighter nucleus and more cytoplasm. In the fractions of medium EPM, most of the small cells were normoblasts which considerably overlapped with small lymphocytes in the size histogram (Fig. 7, 8b). The larger cells were all lymphoid cells with clearly visible cytoplasm which was more prominent in the larger than the smaller cells. The results suggest that 1) cell populations discrete in volume and EPM also show differences in morphology and 2) by means of these cytophysical properties, at least six different lymphoid cell populations can be described: one population in the range of high EPM, three populations in the range of medium EPM and two populations in the range of low EPM.

#### *Proliferative Activity*

The lymphoid cell populations previously characterized may represent populations different with respect to cell cycle phase; i.e. the larger cells may represent S/G<sub>2</sub> phase cells and the smaller cells G<sub>1</sub>/G<sub>0</sub> phase cells. In this case, we would expect that pulse labeling of the cells with

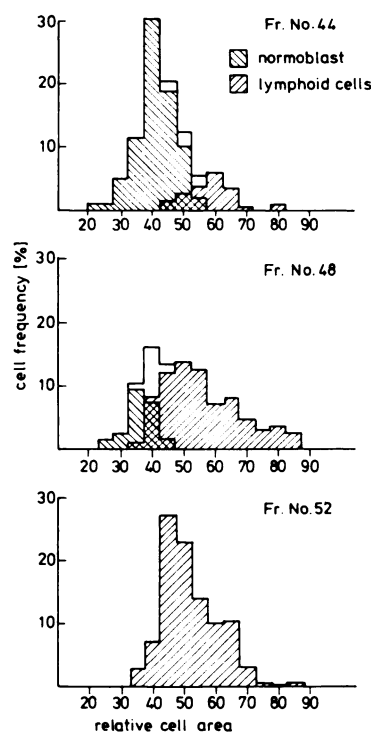
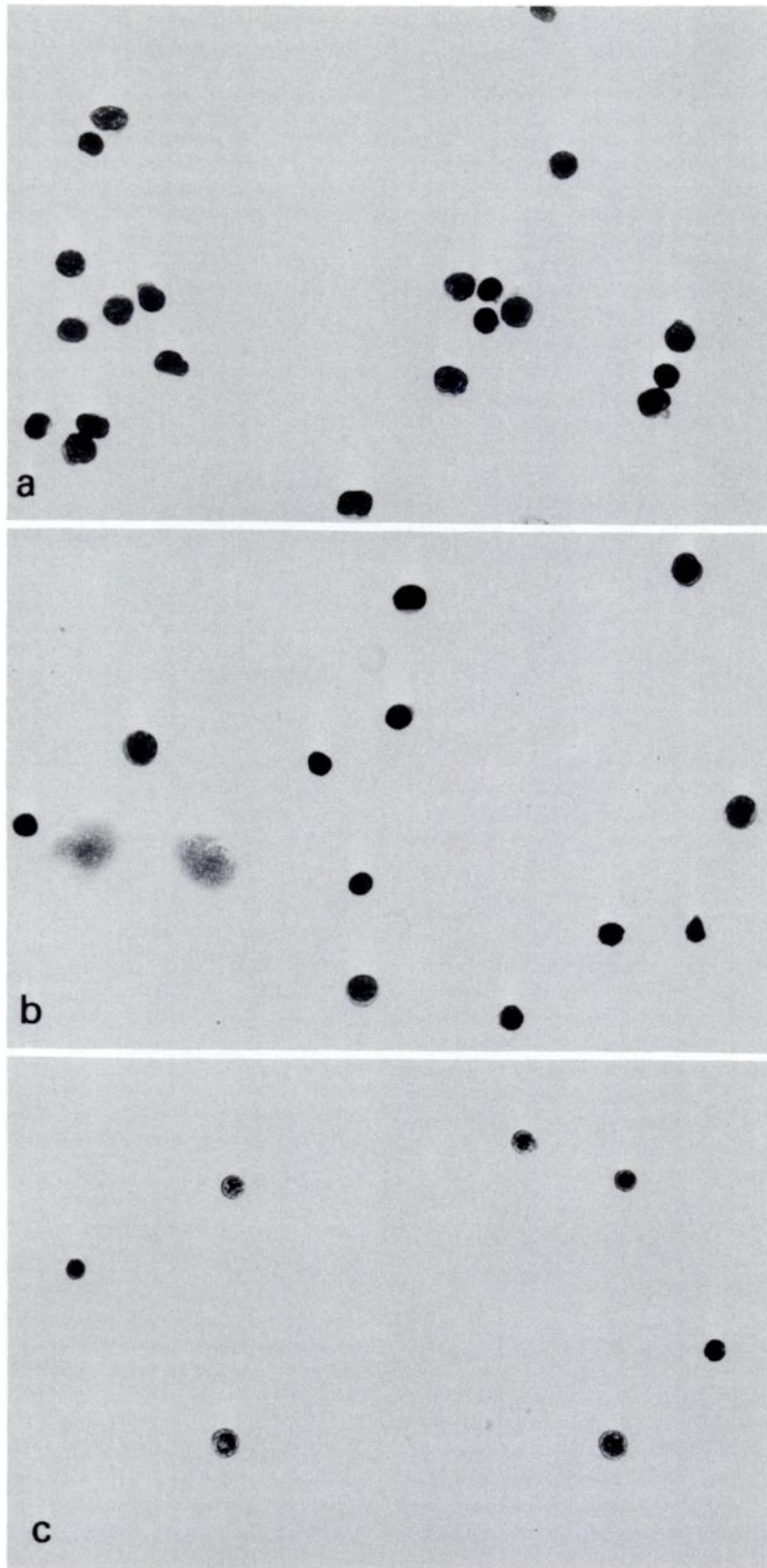


FIG. 7. Area histograms of Giemsa stained cells of different electrophoretic fractions on air-dried and methanol-fixed smears. The cell area is given in arbitrary units.

<sup>14</sup>C thymidine before or after separation would reveal a discrete peak of radioactivity in the respective fractions of the sedimentation and electrophoretic profiles. Figure 9 indicates that



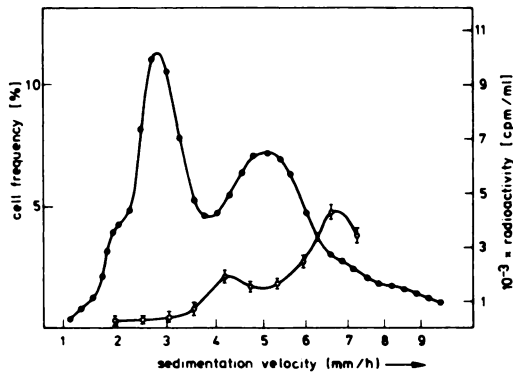


FIG. 9.  $^{14}\text{C}$  thymidine incorporation of  $10^5$  nucleated rat bone marrow cells of different sedimentation velocity (Mean and s.d. are shown). BM = bone marrow; SPL = spleen; Thy = thymus.

up to 3.5 mm/hr, the thymidine incorporation activity was at a negligibly low level but increased with sedimentation velocity showing two discrete peaks at 4.3 mm/hr and 6.8 mm/hr. Electrophoretic separation of the cells sedimenting between 2.6 mm/hr and 3.5 mm/hr also failed to enrich thymidine incorporation activity in any one of the distinct cell peaks. Though we can not rule out that S/G<sub>2</sub> phase cells were selectively damaged in these fractions, it seems more likely that none of the lymphoid cells showing discrete volume and EPM distributions in these fractions represent an S/G<sub>2</sub> phase population.

#### DISCUSSION

Various bone marrow cell populations were characterized by means of a two dimensional separation using velocity sedimentation and electrophoresis, followed by electrical sizing of the fractions and mathematical approximations of normal distributions to the volume profiles. A critical analysis showed that the results obtained are unlikely to be due to experimental artifacts.

In the sedimentation profile of bone marrow cells, up to 4.5 mm/hr, five different cell populations showing discrete distributions in volume and sedimentation velocity were observed. These populations could be roughly correlated with morphologically characteristic cells, i.e. the populations of small size were due to lymphoid cells and normoblasts and the populations of larger size represented myeloid cells. In the faster fractions which contain immature myeloid

and erythroid cells and undefined blast cells, discrete volume distributions were not observed. Thus, in agreement with other authors findings (14, 15, 16), rough separations of different cell lines could be obtained in the range of relatively low sedimentation velocity as a result of discrete differences in average cell volume. However, the resolution obtained is considerably less than that obtained with particles of similar volume distribution but uniform density (13, 28). Apparently bone marrow cells show considerable dispersions in density, causing a several fold larger sedimentation dispersion than found with particles of uniform density. There are two possibilities: 1) Cells of homogeneous size consist of various discrete populations of different average density, and 2) One population shows a large density dispersion which is not correlated with the volume variation. The first possibility is supported by the observation that small lymphocytes and normoblasts are the same size but have different sedimentation velocities. Moreover, small sized bone marrow lymphocytes are composed of various discrete populations of widely differing density (11). The second situation has been shown to exist in a growing lymphocyte line by Splinter and Reiss (21) by using a two-dimensional separation analysis by means of velocity sedimentation and buoyant density centrifugation. These aspects have been reviewed in detail by Pretlow (17). In summary it seems that the separated cell populations of homogeneous size in the slowly sedimenting fractions represent a cell mixture of considerable heterogeneity.

In the faster fractions, different cell volumes are shown not only by different cell lines but also by different cell cycle phases within these lines. This was revealed by pulse labeling of the cells in the separated fractions with  $^{14}\text{C}$  thymidine which indicated a characteristic bimodal incorporation activity profile in the fractions faster than 3.5 mm/hr. Since cells double their volume in S/G<sub>2</sub> phase, the daughter cells of the labeled cells sediment with slower velocity. Therefore we expect a considerable overlap of different cell lines and cycle phases in the faster fractions. In fact the volume profiles of the cells in these fractions are not discrete and show an excessively broad coefficient of variation. Nevertheless, the volume distributions of single populations are discrete as suggested by the bimodal

FIG. 8a-c. Photomicrographs of Giemsa stained bone marrow cells of different electrophoretic mobility in: a) fraction No. 44; b) fraction No. 48; c) fraction No. 52 of the profile shown in Figure 5.  $\times 500$ .

profile of S phase cells. This is in close agreement with the observations of Valet *et al.* (23) that the cycle phases of bone marrow cells each show different discrete volume clusters. In summary it appears that the broad dispersion in density and volume within different bone marrow cell lines considerably restricts the preparative value of velocity sedimentation. Nevertheless this method is of great value from an analytical point of view since the volume dispersion of a cell of known function can be indirectly determined (12, 13). Within the cells sedimenting slower than 3.5 mm/hr, further resolution was achieved by free flow electrophoresis.

These cells consist of a majority of lymphoid cells, the remainder being small normoblasts. Before electrophoresis, the cells fall into three different discrete volume distributions of small, medium and larger size. After separation, the small and medium sized cells each showed a peak in the fractions of low, medium and high EPM while the larger cells showed a single peak in the fractions of medium EPM. The electrophoretic profiles of the small sized populations in the range of high and medium EPM were due to normoblasts whereas the other populations represented lymphoid cells. Within these lymphoid cells, size distributions could be correlated with characteristic morphology which was particularly evident in the fractions of low and high EPM.

Thus it may be that the BM lymphocyte populations defined by volume and EPM each represent biologically characteristic cells. This is supported by the observations that: 1) the small sized population of low EPM carry thymus-specific antigens (26) and respond to Con A mitogen (6), and 2) that the electrophoretic distribution of the size-defined BM lymphocytes agrees well with that of functionally different lymphocytes in peripheral lymphoid organs (5, 27, 31). Moreover, it seems rather unlikely that a biologically unspecific effect would give rise to such a pronounced discreteness in the distribution of two causally uncorrelated properties such as volume and EPM. The finding of Ruhenstroth-Bauer *et al.* (18) that rat thoracic duct lymphocytes fall into two normal volume distributions and are different in EPM and X-ray sensitivity lends support to the idea that specific cytophysical parameters have a biological meaning. Discrete normal volume distributions have also been observed in blood and thoracic duct leukocytes of

other species (9, 19, 25). These results agree with the observations in homogeneous culture cell lines which showed that the volume variation is an inherent and characteristic cell property (3). Our results show that in a mixed cell population, volume alone is not a specific cell marker; however, when combined with another parameter its value is considerably enhanced.

In general it seems that multi-dimensional cell separations combined with the analysis of cytophysical parameters is not only a promising approach to improving the resolution in preparative separation but may also be valuable in the characterization of biologically different cell populations on a per cell basis in a rapid way.

#### ACKNOWLEDGMENTS

We thank Prof. K. Hannig for his generous support of the work and Drs. G. Pascher and G. Valet for their help and valuable discussion. The technical assistance of Mrs. C. Eckelt and Miss R. Wiemeyer is gratefully acknowledged. This work was supported by the SFB 37 of the Deutsche Forschungsgemeinschaft.

#### LITERATURE CITED

1. Anderson EC, Bell GI, Petersen DF, Tobey RA: Cell growth and division. Determination of volume growth rate and division probability. *Biophys J* 9:246, 1969
2. Ben-Sasson S, Patinkin D, Grover NB, Doljanski F: Electrical sizing of particles in suspensions. *J Cell Physiol* 84:205, 1974
3. Buckhold B, Shank B, Burki HJ: Surface charge and cell volume of synchronized mouse lymphoblasts (L 5178-Y). *Cell Physiol* 78:243, 1971
4. Doljanski F, Benn-Sasson S, Reich M, Grover NB: Dynamic osmotic behavior of chick blood lymphocytes. *J Cell Physiol* 84:215, 1974
5. Hannig K, Zeiller K: Zur Auftrennung und Charakterisierung immunkompetenter Zellen mit Hilfe der trägerfreien Ablenkungselektrophorese. *Hoppe-Seyler's Z Physiol Chem* 350:467, 1969
6. Hansen E: Separation und Charakterisierung von Knochenmarkslimphozyten der Ratte. Diplomarbeit, Ludwig-Maximilian Universität München, 1975
7. Hendil KB, Hoffmann EK: Cell volume regulation in Ehrlich ascites tumor cells. *J Cell Physiol* 84:115, 1974
8. Hilal SK, Mosser DG, Loken MK, Johnson RW: New technique for high-resolution density gradient-separation of bone marrow cells. *Ann NY Acad Sci* 114:661, 1964
9. Humphries RK, Miller RG: Volume analysis of human peripheral blood leucocytes. *Ser Haematol* 5:142, 1972
10. Kachel V: Basic principles of electrical sizing of

- cells and particles and their realization in the new instrument "Metricell". *J Histochem Cytochem* 24:211, 1976
11. Leif RC, Smith SB, Warters RL, Dunlap LA, Leif SB: Buoyant density separation of cells. The buoyant density distribution of guinea pig bone marrow cells. *J Histochem Cytochem* 23:378, 1975
  12. MacDonald HR, Miller RG: Synchronization of mouse L-cells by a velocity sedimentation technique. *Biophys J* 10:835, 1970
  13. Miller RG, Phillips RA: Separation of cells by velocity sedimentation. *J Cell Physiol* 73:191, 1969
  14. Moon R, Phillips RA, Miller RG: Sedimentation and volume analysis of human bone marrow. *Ser Haematol* 5:163, 1972
  15. Osmond DG, Miller RG, Boehmer H: Characterization of immunoglobulin-bearing and other small lymphocytes in mouse bone marrow by sedimentation and electrophoresis. *J Immunol* 114:1230, 1975
  16. Petersen EA, Evans WH: Separation of bone marrow cells by sedimentation at unit gravity. *Nature* 214:824, 1967
  17. Pretlow TG, Weir EE, Zettergren IG: Problems connected with the separation of different kinds of cells. *Int Rev Exp Pathol* 14:91, 1975
  18. Ruhenstroth-Bauer G, Lücke-Huhle CJ: Two populations of small lymphocytes. *J Cell Biol* 37:196, 1968
  19. Sipe CR, Chanana AD, Cronkite EP, Joel DD, Schiffer LM: Studies on lymphopoiesis. Size distribution of bovin thoracic duct lymphocytes. *Proc Soc Exp Biol Med* 123:158, 1966
  20. Spielman L, Goren SL: Improving resolution in coulter counting by hydrodynamic focusing. *J Coll Sci* 26:175, 1968
  21. Splinter TAW, Reiss M: Separation of lymphoid-line cells according to volume and density. *Exp Cell Res* 89:343, 1974
  22. Thom R, Hampe A, Sauerbrey G: Die elektronische Volumenbestimmung von Blutkörperchen und ihre Fehlerquellen. *Z Gesamte Exp Med* 151:331, 1969
  23. Valet G, Hanser G, Ruhenstroth-Bauer G: Simultaneous measurement of the volume and DNA content of rat bone marrow cells by the Fluvo-Metricell flow cytometer. Third international symposium on "Pulse cytophotometry", Wien (1977) Submitted for publication
  24. Valet G, Hofmann H, Ruhenstroth-Bauer G: The computer analysis of volume distribution curves. Demonstration of two erythrocyte populations of different size in the young guinea pig and analysis of the mechanism of immune lysis of cells by antibody and complement. *J Histochem Cytochem* 24:231, 1976
  25. Westring DW, Ladinsky JL, Feick P: The volume distribution of human lymphocytes. *Proc Soc Exp Biol Med* 131:1077, 1969
  26. Zeiller K, Dolan L: Study of cell surface antigens on electrophoretically separated rat lymphocytes. Tracing of the differentiation pathway of bone marrow-derived thymocytes by use of a surface marker. *Eur J Immunol* 2:439, 1972
  27. Zeiller K, Hannig K, Pascher G: Free-flow electrophoretic separation of lymphocytes. Separation of graft *versus* host reactive lymphocytes of rat spleens. *Hoppe-Seyler's Z Physiol Chem* 352:1168, 1971
  28. Zeiller K, Hansen E, Leihener D, Pascher G, Hannig K: Analysis of velocity sedimentation techniques in cell separation. Influence of apparatus and sample properties on separative power, resolution and sensitivity. *Hoppe Seylers Z Physiol Chem* 357:1309, 1976
  29. Zeiller K, Holzberg E, Pascher G, Hannig K: Free-flow electrophoretic separation of T and B lymphocytes. Evidence for various subpopulations of B cells. *Hoppe Seylers Z Physiol Chem* 353:105, 1972
  30. Zeiller K, Löser R, Pascher G, Hannig K: Free flow electrophoresis. Analysis of the method with respect to preparative cell separation. *Hoppe Seylers Z Physiol Chem* 356:1225, 1975
  31. Zeiller K, Pascher G, Hannig K: Preparative electrophoretic separation of antibody-forming cells. *Prep. Biochemistry* 2:1, 1972
  32. Zeiller K, Schubert JCF, Walther F, Hannig K: Free-flow electrophoretic separation of bone marrow cells. Electrophoretic distribution analysis of *in vivo* colony forming cells in mouse bone marrow. *Hoppe Seylers Z Physiol Chem* 353:95, 1972